Title

A Charge Injection Loss Compensation Method for a Series-Stacked Buffer to Reduce Current and Voltage Ripple in Single-Phase Systems

Authors

Fernandez, Kelly
Brooks, Nathan
Ge, Ting
et al.

Publication Date

2022-03-24

DOI

10.1109/apec43599.2022.9773672

Peer reviewed

2022 IEEE Applied Power Electronics Conference and Exposition (APEC), Houston, TX, USA, March 2022

A Charge Injection Loss Compensation Method for a Series-Stacked Buffer to Reduce Current and Voltage Ripple in Single-Phase Systems

K. Fernandez
N. Brooks
T. Ge
Z. Liao
R. C. N. Pilawa-Podgurski

A Charge Injection Loss Compensation Method for a Series-Stacked Buffer to Reduce Current and Voltage Ripple in Single-Phase Systems

Kelly Fernandez, Nathan Brooks, Ting Ge, Zitao Liao, Robert C.N. Pilawa-Podgurski
email: kefernandez@berkeley.edu

***Abstract*—Single-phase rectifier and inverter applications require an additional reactive circuit branch tied to the dc-link in order to remove the twice line frequency power pulsation that couples to the dc bus. The series-stacked buffer (SSB) has been identified as an active buffer topology that buffers this reactive power with a high energy utilization factor. However, the SSB requires an additional loss compensation control that injects real power into the SSB branch. Consequently, residual ac current and voltage ripple remain coupled to the dc-link. This paper proposes a novel loss compensation method featuring augmented hardware and control that introduces charge injection which eliminates this twice line frequency ripple from the dc-link. A 1.5 kW hardware prototype was built and tested to verify the effectiveness of the newly proposed charge injection method.**

I. Introduction

Single-phase rectifier and inverter systems contain a twice-line frequency power pulsation that is coupled to the dc bus due to the mismatch in instantaneous power between the ac and dc ports. To remove the twice-line frequency ripple from the dc bus, large dc-link capacitors or additional active filters are typically employed [**?**]. Active buffers are becoming increasingly popular solutions due to improvements in the energy utilization factor of the reactive energy storage components, the overall system volume, and the cost in comparison to bulky solutions utilizing electrolytic capacitors [**?**], [**?**], [**?**], [**?**]. Specifically, capacitor-based active buffer solutions further improve system power density since the energy density of capacitors can be up to two orders of magnitude higher than inductors [**?**]. One capacitive-based active buffer topology in particular, the Series-Stacked Buffer (SSB), has been shown to be highly efficient, to have high energy utilization, and to achieve smaller volume than both passive and other active buffer solutions [**?**], [**?**], [**?**], [**?**]. Fig. 1 displays the system model of a SSB that is connected to a dc voltage source with source impedance R_s and an output inverter stage modeled with current

$$I_{inv} = I_{DC}\sin(\omega_{2L}t) + I_{DC}, \tag{1}$$

where ω_{2L} is the system's angular twice-line frequency $2 \cdot (2\pi f_L)$ and f_L is the nominal ac mains' frequency of either 50 or 60 Hz. Assuming no power losses, I_{DC} is the dc-offset of input current I_{in}. The associated waveforms of the modeled 1.5 kW rated SSB system model with a source impedance of R_s = 10 Ω are also displayed in Fig. 1.

Although the SSB buffers the majority of the dc-link's twice-line frequency power pulsation ripple, a drawback of the SSB is the residual twice-line frequency ripple that is left coupled to the dc-link due to the SSB's required loss compensation control. As described in Section II, the loss compensation control introduces a twice-line frequency ripple to both V_{bus} and I_{in} that is dependent on source impedance R_s and the power losses of the SSB. This residual ac ripple on the dc-link can be seen in Fig. 1, where the dc input current ripple is greater than 10% of the average current. This ripple is larger for dc sources with smaller source impedance. Thus, while this is not a problem in systems with relatively large R_s, such as in a photovoltaic application presented in [**?**], for systems with small R_s, such as in battery systems where R_s can be less than 1 Ω [**?**], the corresponding ripple can be a limiting factor in the SSB's effectiveness in buffering energy.

In this work we present a new charge injection technique that can provide loss compensation to the SSB that provides substantial reduction to dc-side ripple. The new charge injection method has the potential to entirely remove the twice-line frequency power pulsation on the dc-link by decoupling the reactive power and real power flow of the SSB through the addition of another circuit branch and control loop. Test results with a 1.5 kW hardware prototype demonstrating improvements in the current ripple and compare the efficiencies between the charge injection and previous control method are included.

II. Principles of Operation

A. Ideal SSB Operation

The schematic presented in Fig. 1 is the SSB architecture connected in parallel with dc source V_{DC} and a modeled inverter load as described in [**?**]. Capacitor C_1 acts as the main energy storage capacitor for the dc-link and is allowed to have relatively large ac ripple. Assuming that there is no power loss in the SSB converter, the voltage across C_1 is

$$v_{C1}(t) = V_{bus} + \frac{I_{DC}}{\omega_{2L}C_1}\cos(\omega_{2L}t) = V_{bus} + v_{C1,ac}(t). \tag{2}$$

An H-bridge converter, with capacitor C_2 acting as its dc voltage source, is placed in series with C_1. Assuming no losses, the H-bridge converter can be controlled to produce an ac output voltage v_{ab} = - $v_{C1,ac}(t)$. Effectively, V_{bus} is purely dc and the power processed by the SSB is purely reactive. In

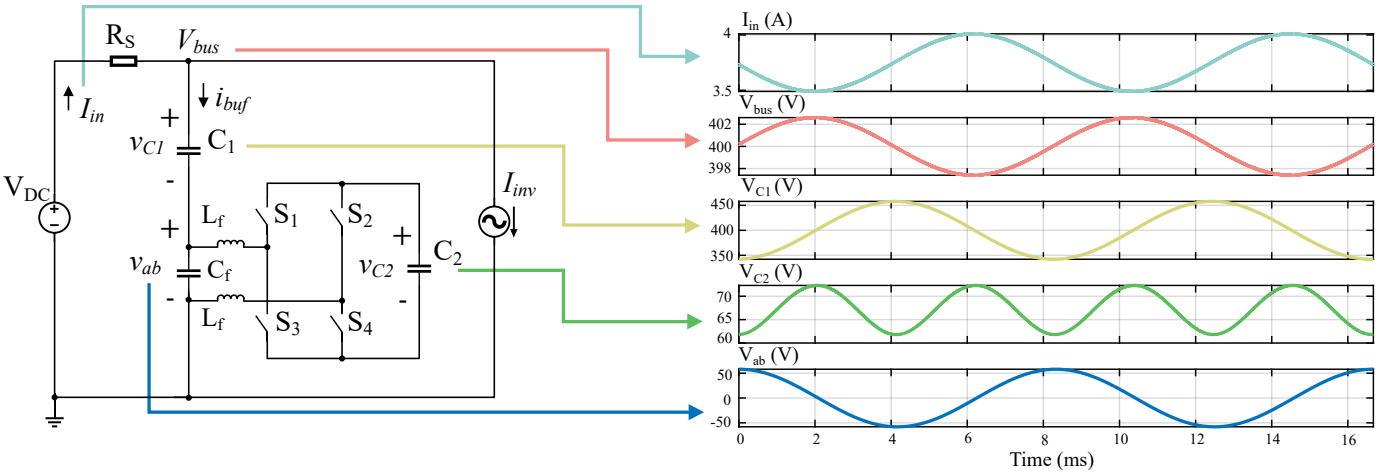

Fig. 1: Schematic of a traditional series-stacked buffer converter connected to a dc voltage source V_{DC} and a modeled inverter current load I_{inv}. Voltage and current waveforms of the system are displayed for a 1.5 kW system operation where $V_{bus,dc}$ = 400 V, I_{DC} = 3.75 A, C_1 = 80 μF, C_2 = 204 μF, and R_s = 10 Ω.

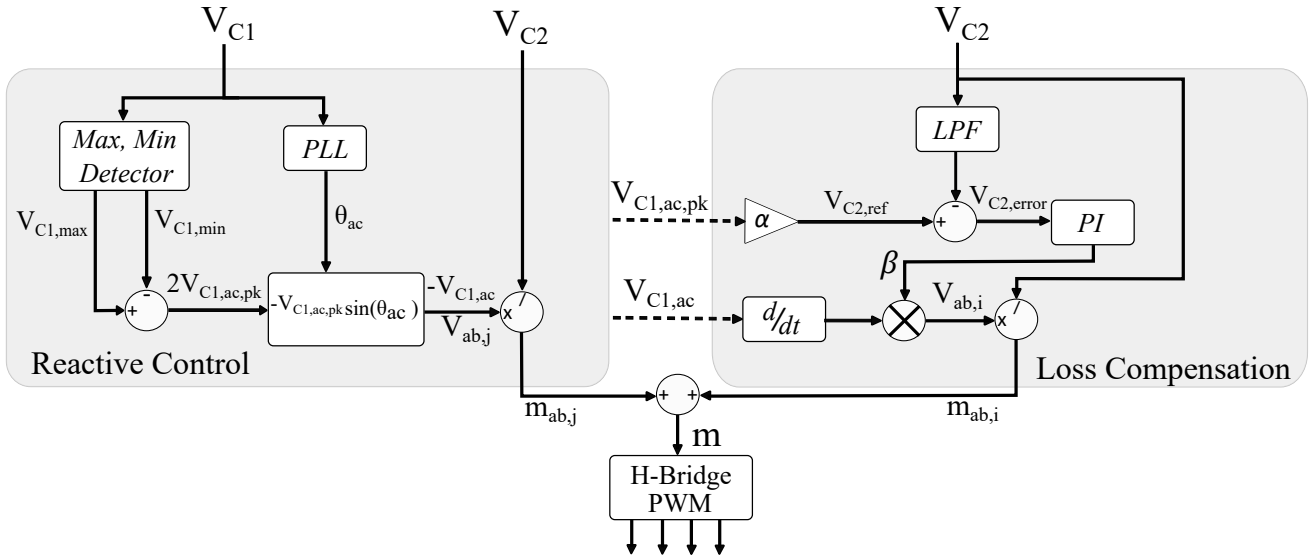

Fig. 2: Control diagram for a SSB implemented with a traditional loss compensation control.

this case, the twice-line frequency ripple coupled to I_{in} and V_{bus} in Fig. 1 would be reduced to zero. In a hypothetically lossless system, ideal SSB operation is achieved by the control and sensing that is described in the reactive control block of Fig. 2.

B. SSB Loss Compensation

In a hardware circuit implementation, the assumption of zero losses in the H-bridge converter does not hold. As a result, C_2 continuously loses charge and decays in voltage. This prevents the SSB from buffering the twice-line frequency power pulsation that is coupled to the dc-link. System waveforms of the SSB with no loss compensation control are shown in Fig. 3. Before t = 0 seconds, capacitors C_1 and C_2 are initially charged to their steady-state dc voltage offsets for a 1.5 kW system operation. At t = 0 seconds, the system turns on and the average of v_{C2} begins to decay. This causes v_{ab} to saturate and prevents the SSB from buffering the dc-link's ac ripple. To prevent this from happening, loss compensation control is required in order to keep C_2 charged. The loss compensation block in the control diagram of Fig. 2 can be implemented in order to inject real power into C_2 through the reactive buffer branch. However, allowing real power to flow through the SSB branch causes an undesirable phase shift for v_{ab} [**?**]. Effectively, the sum $v_{C1} + v_{ab}$ is no longer strictly dc and leaves a residual amount of ac voltage ripple coupled to V_{bus}. This causes ac current ripple to become coupled to I_{in} that can negatively impact system operation. Following the impedance modeling in [**?**], and by knowing load current I_{inv}, I_{in} can be approximated as follows:

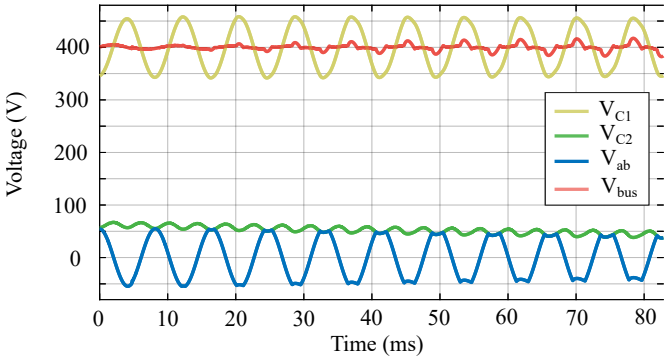

Fig. 3: SSB system waveforms when no loss compensation control is implemented.

$$I_{in}(t) = I_{DC} + I_{DC}\frac{R_{ab}}{R_s + R_{ab}}\sin(\omega_{2L}t) = I_{in,dc} + I_{in,ac}\sin(\omega_{2L}t). \quad (3)$$

where R_{ab} is the effective series resistance in the reactive branch due to the power losses of the SSB converter. As shown in (3), the dc ripple current $I_{in,ac}$ is dependent on the power losses of the H-bridge converter and source impedance R_s. However, R_s is often a fixed parameter based on the input dc source that cannot be adjusted. In particular for sources with voltage-source behavior (e.g., batteries), the very low R_s makes the loss compensation technique difficult to utilize in practice.

III. Charge Injection

The schematic and the control diagram for the proposed charge injection method are displayed in Figs. 4 and 5. The charge injection circuitry is an additional circuit branch that consists of switch S_{CI}, inductor L_{ci}, and diode D_{CI}. The charge injection branch periodically connects the dc-link to capacitor C_2 in order to directly deliver real power. This charge injection method decouples the reactive and real power handling in both hardware and control. As a result, the H-bridge can be precisely modulated to ensure that $v_{ab} = -v_{C1,ac}$ and to minimize the twice-line frequency voltage ripple coupled to V_{bus}, which greatly reduces the amplitude of $I_{in,ac}$. This is shown in the simulated waveforms of Fig. 4, where $I_{in,ac}$ is reduced by a factor of five in comparison to the traditional loss compensation method simulation shown in Fig. 1.

A. Reactive Power Control

The primary operation of the reactive power control of the SSB with the charge injection method remains mostly the same as in the previous section. The main difference between the reactive power control of the two loss compensation methods is the unipolar modulation scheme for the H-bridge. In the traditional unipolar modulation scheme described in [**?**], the H-bridge shorts the ac output by conducting switches S_1 and S_2 simultaneously, or by conducting switches S_3 and S_4 simultaneously. However, the simultaneous conduction of switches S_1 and S_2 is undesirable for the charge injection method because when these switches are both on, there is no closed loop path for the charge injection circuit to deliver charge to C_2. Conversely, during the simultaneous conduction of switches S_3 and S_4, there is a closed loop path for the charge injection circuit to deliver charge to C_2. Therefore, to ensure that charge can be delivered each switching cycle to C_2, a new unipolar modulation scheme was created for the H-bridge that eliminates the S_1 and S_2 simultaneous conduction state. The duty cycle for switches S_1 and S_2 are calculated from modulation index m as follows:

$$\begin{aligned} m > 0 \quad (v_{ab} > 0 \text{ V}): \quad & d_{S1} = |m|,\ d_{S2} = 0 \\ m < 0 \quad (v_{ab} < 0 \text{ V}): \quad & d_{S1} = 0,\ d_{S2} = |m|. \end{aligned} \quad (4)$$

When v_{ab} is regulated to be larger than 0 V, switch S_4 is turned on and the switches S_1 and S_3 are modulated complimentary with duty cycle d_{S1} equal to m. Therefore during this (positive) half of the twice-line frequency cycle, only the simultaneous conduction of switches S_1 and S_4 or switches S_3 and S_4 are permitted. Similarly, when v_{ab} is regulated to be less than 0 V, switch S_3 is turned on and the switches S_2 and S_4 are modulated complimentary with duty cycle d_{S2} equal to the absolute value of m. Therefore during this (negative) half of the twice-line frequency cycle, only the simultaneous conduction of switches S_2 and S_3 or switches S_3 and S_4 are permitted. As a result, the undesired circuit state where S_1 and S_2 are simultaneously conducting is avoided completely and charge can be injected into C_2 through the charge injection circuitry over the entire twice-line period.

B. Charge Injection Loss Compensation Control

At an abstracted level, the charge injection methodology can be considered as a buck converter with a voltage feedback loop that monitors $v_{C2,dc}$ and drives capacitive load C_2. To ensure that there is sufficient charge stored in C_2, a reference value related to the capacitor's dc voltage $v_{C2,dc}$ is obtained. As described in [**?**], the reference value for $v_{C2,dc}$ is the product

$$v_{C2,dc,ref} = \sqrt{\frac{2C_2 + C_1}{2C_2}}\, v_{C1,ac,pk} = \alpha \cdot v_{C1,ac,pk}, \quad (5)$$

where $v_{C1,ac,pk}$ is the amplitude of the twice-line frequency ac ripple of v_{C1} and variable α represents the constant square root term shown in (5). The error $v_{C2,dc,ref} - v_{C2,dc}$ is fed into a PI voltage compensator. The output of the compensator is the duty cycle for the charge injection switch S_{CI}.

The charge injection circuit is purposefully designed to operate in discontinuous conduction mode (DCM) due to C_2 requiring a small amount of real power injection each switching period. Therefore, when both switch S_{CI} and diode D_{CI} are off, there is no current through any of the charge injection components and therefore there is no real power delivered to C_2. When switch S_{CI} turns on, current through inductor L_{CI} begins to increase linearly from 0 A and delivers charge to C_2. Note, some of the inductor L_{CI} current is transmitted to the upper filter inductor L_f that is connected to the same node as the positive terminal of C_2. The slope of the inductor current i_{Lci} can be calculated based on the voltage

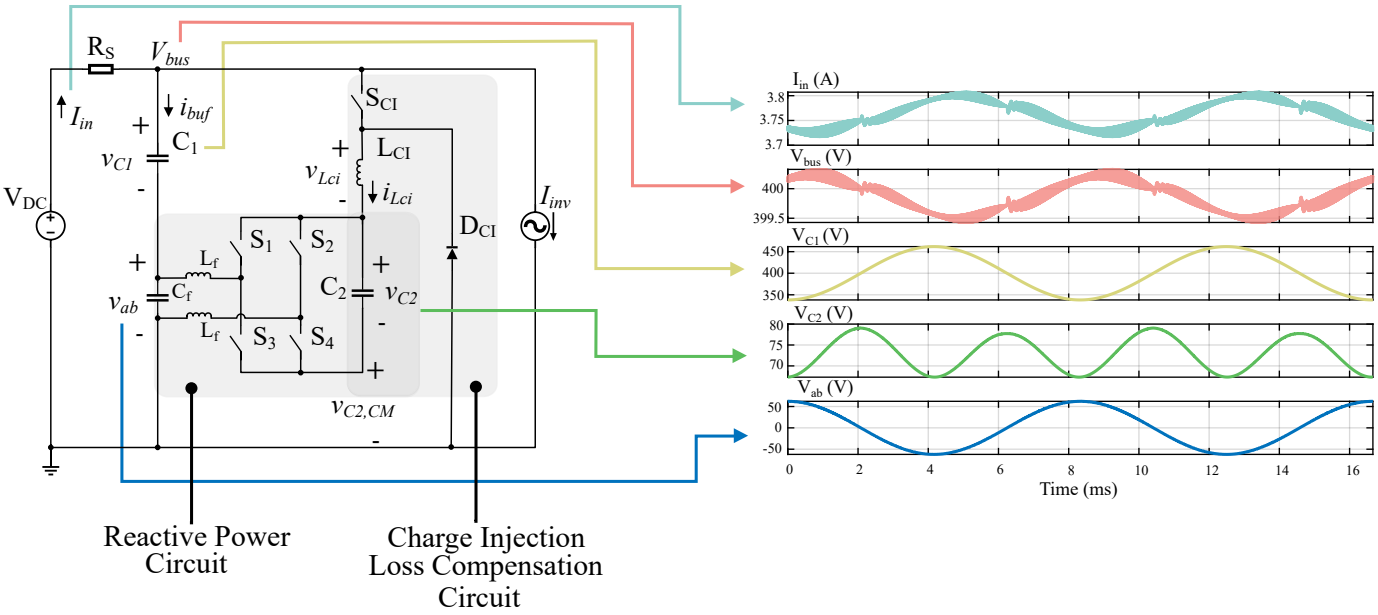

Fig. 4: Schematic of a SSB with charge injection method connected to a dc voltage source and a modeled inverter current load. Voltage and current waveforms of the system are displayed for a 1.5 kW system operation where $V_{bus,dc}$ = 400 V, I_{DC} = 3.75 A, C_1 = 80 μF, C_2 = 204 μF, and R_s = 10 Ω.

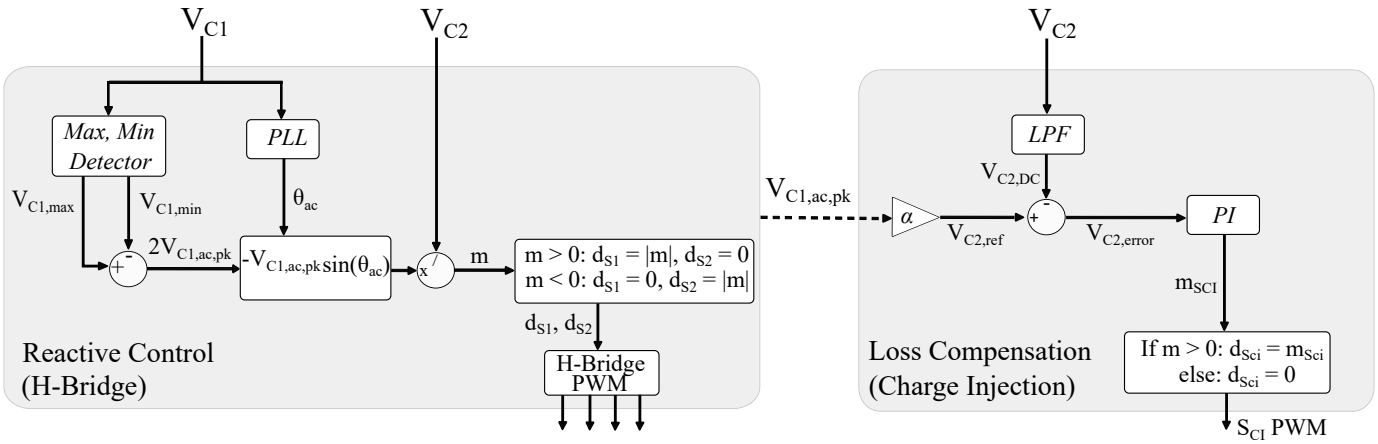

Fig. 5: Control diagram for an SSB implemented with charge injection loss compensation control.

across L_{CI}:

$$v_{Lci} = V_{bus} - (v_{C2} + v_{C2,CM}), \tag{6}$$

where V_{bus} is the dc-link voltage, v_{C2} is voltage across C_2, and $v_{C2,CM}$ is the common-mode voltage of C_2. The common-mode voltage $v_{C2,CM}$ is dependent on the H-bridge's circuit state of operation. Thus, although the control between the reactive and real branches of the SSB are decoupled from one another, the H-bridge's switching state affects the rate of the charge delivered to C_2. Moreover, the orientation of v_{ab} affects the common mode voltage of C_2 and therefore also affects the rate of the charge delivered to C_2. To better understand the shape of the current i_{Lci}, the SSB can be divided into twelve different circuit states that depend on the orientation of v_{ab}, the switching state of the H-bridge, and the switching state of the charge injection circuit. Table I displays the twelve different SSB circuit states and the effective voltage v_{Lci}.

When the charge injection switch S_{CI} turns off, diode D_{CI} is forced to conduct to freewheel the current through the inductor L_{CI} and the H-bridge's filter inductors L_f. The inductor L_{CI} is now connected to the ground of the circuit and the voltage across the inductor v_{Lci} is now negative, which causes the current through the inductor to decrease. Once the inductor current reaches 0 A, all of the elements in the charge injection circuit are no longer conducting current, and the charge injection circuit is effectively turned off until the next switching period.

TABLE I: Series-Stacked Buffer with Charge Injection Circuit States of Operation

State	V_{ab} orientation	H-bridge Switches	S_{CI}	D_{CI}	V_{Lci}
I	positive	S_3 and S_4 on	off	off	n/a
II	positive	S_1 and S_4 on	off	off	n/a
III	positive	S_1 and S_4 on	on	off	$V_{bus} - 0.5\,(V_{ab} + V_{C2})$
IV	positive	S_1 and S_4 on	off	on	$-0.5\,(V_{ab} + V_{C2})$
V	positive	S_3 and S_4 on	on	off	$V_{bus} - 0.5\,(V_{ab} + 2V_{C2})$
VI	positive	S_3 and S_4 on	off	on	$-0.5\,(V_{ab} + 2V_{C2})$
VII	negative	S_3 and S_4 on	off	off	n/a
VIII	negative	S_2 and S_3 on	off	off	n/a
IX	negative	S_2 and S_3 on	on	off	$V_{bus} - 0.5\,(V_{ab} + V_{C2})$
X	negative	S_2 and S_3 on	off	on	$-0.5\,(V_{ab} + V_{C2})$
XI	negative	S_3 and S_4 on	on	off	$V_{bus} - 0.5\,(V_{ab} + 2V_{C2})$
XII	negative	S_3 and S_4 on	off	on	$-0.5\,(V_{ab} + 2V_{C2})$

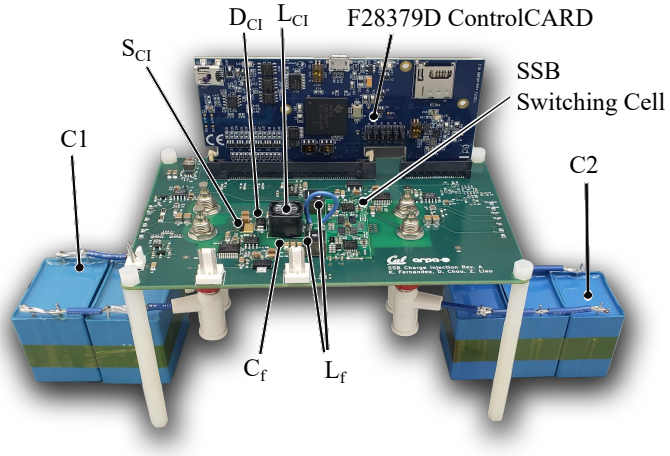

Fig. 6: Hardware prototype of the SSB with charge injection method that is rated for 1.5 kW. A list of components used in the prototype can be found in Table II.

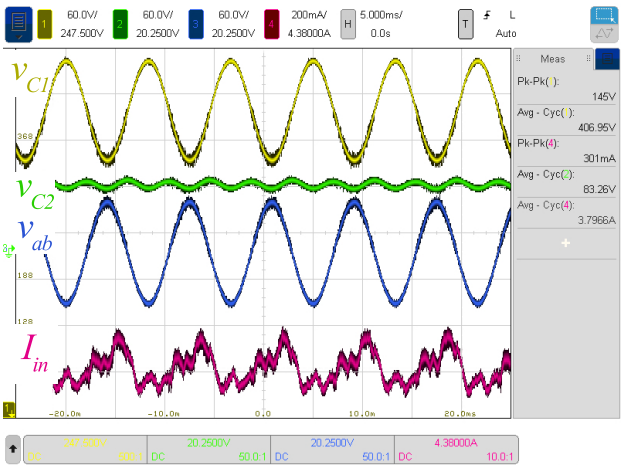

Fig. 7: Steady state waveforms of v_{C1} (yellow), v_{C2} (green). v_{ab} (blue) and I_{in} (pink) at 1.5 kW with $V_{bus,dc}$ = 400 V.

TABLE II: Component Listing

Component	Part No.	Parameters
S_1, S_2, S_3, and S_4	EPC 2033	150 V, 7 mΩ
S_{CI}	GaN Systems GS66506T	650 V, 67 mΩ
D_{CI}	ON Semiconductor MURS160T3G	600 V, 2 A
L_{CI}	Coilcraft MSS1210-104	100 μH
L_f	Coilcraft XAL7070-473	47 μH x 2
C_1	TDK B32524Q1686K000	100 V, 68 μF x 3
C_2	TDK B32776G4406K000	450 V, 40 μF x 2

IV. Experimental Results

A 1.5 kW series-stacked buffer hardware prototype was designed and built to validate the charge injection loss compensation method. The control for the prototype was implemented digitally using a TI C2000 F28379D ControlCARD. The hardware prototype is displayed in Fig. 6 and the components used in the prototype are listed in Table II. The prototype was tested using both the charge injection method and the traditional SSB loss compensation method up to 1.5 kW with a rated dc bus of $V_{bus,dc}$ = 400 V. A MagnaPower TSD1000 was used for the dc power supply V_{DC} and a Chroma 63204 DC electronic load was used for the output inverter-modeled load I_{inv}.

Fig. 7 shows the steady state waveforms for the SSB with charge injection method at 1.5 kW and $V_{bus,dc}$ = 400 V. The waveforms for v_{C1}, v_{C2}, and v_{ab} are consistent with the simulated waveforms shown in Fig. 4. However, the input dc current I_{in} still contains minor twice-line frequency ripple. This may be a byproduct of errors associated with the analog-to-digital converter (ADC) sensing of v_{C1}, error in the phase-locked loop (PLL) output θ, and the propagation delay between the ADC sensing, micro-controller, and gate signal of the H-bridge switches. To further reduce the peak-to-peak ripple of the dc input current, the sensing circuitry can be improved upon and a more advanced PLL, such as the second-order generalized integrator (SOGI) PLL [**?**], can be used.

A 1.5 kW to 750 W load step is shown in Fig. 8, validating the stability of both the H-bridge and charge injection control loops. Fig. 9 displays the efficiency and peak-to-peak input

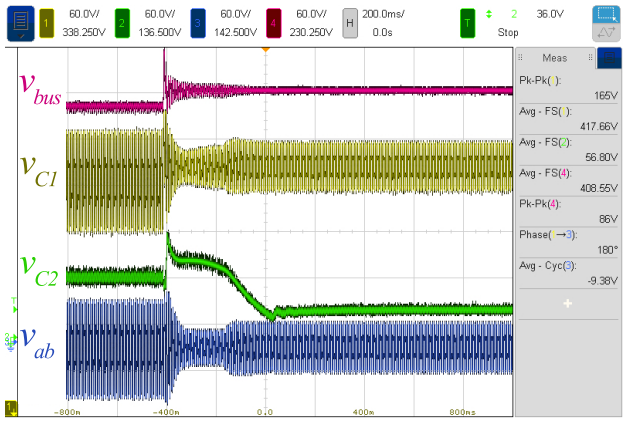

Fig. 8: Waveforms of the SSB with charge injection method captured during a load step from 1.5 kW ($V_{bus,dc}$ = 400 V) to 750 W.

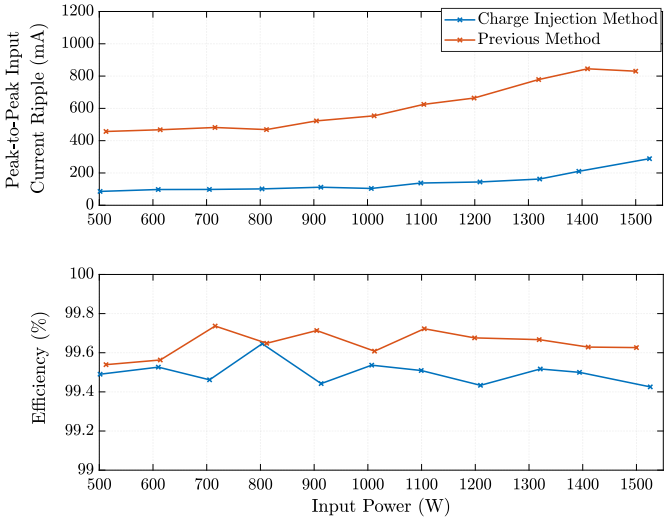

Fig. 9: The peak-to-peak dc input current ripple and efficiency comparisons between the previous loss compensation method highlighted in Section II, and the charge injection method.

current ripple of both the charge injection method and the traditional loss compensation method over a range of input power levels. Voltage, power, and current measurements of V_{bus}, I_{in}, and I_{inv} were recorded with a Keysight PA2203A over a time span of ten twice-line frequency cycles. The input and output power of both methods was averaged over the ten twice-line cycles to calculate each method's efficiency at different power levels. The maximum and minimum of the input current I_{in} was recorded over ten twice-line cycles to calculate the peak-to-peak input dc current ripple.

The peak-to-peak dc current ripple measured in the charge injection method is consistently four times lower than the ripple of the traditional loss compensation method. The peak ripple reduction is achieved at 1 kW, where the charge injection method's peak-to-peak input current ripple is more than five times smaller than the ripple of the traditional method. However, the efficiency of hardware using the charge injection method is smaller than that of the previous loss compensation method. It is expected that the majority of the power loss in the charge injection circuitry is due to the conduction losses associated with diode D_{CI}. Secondary contributors of power loss include the hard switching and conduction losses of switch S_{CI} and the DCR of L_{CI}.

V. Conclusion

This work describes how the traditional loss compensation control for a series-stacked buffer buffer causes an undesirable, residual twice-line frequency current and voltage ripple along the dc-link of the electrical system. To mitigate this ripple, the proposed charge injection method effectively decouples the reactive power buffering from the real power loss compensation and enables dc-link current and voltage ripple minimization. This is accomplished with the introduction of a separate real power loss compensation circuit branch and a decoupled control loop. A proof-of-concept 1.5 kW hardware prototype was built to showcase the charge injection method. Results up to 1.5 kW verified the charge injection method's ability to reduce the twice-line frequency dc current and voltage ripple with some decrease in efficiency in comparison to the traditional loss compensation method. Suggestions to further improve the charge injection's efficiency are also given.

VI. Acknowledgement

This material is based upon work supported by the National Science Foundation Graduate Research Fellowship Program under Grant No. DGE 1752814. Any opinions, findings, and conclusions or recommendations expressed in this material are those of the author(s) and do not necessarily reflect the views of the National Science Foundation.

The information, data, or work presented herein was funded in part by the Advanced Research Projects Agency-Energy (ARPA-E), U.S. Department of Energy, under Award Number DE-AR0000900 in the CIRCUITS program monitored by Dr. Isik Kizilyalli. The views and opinions of authors expressed herein do not necessarily state or reflect those of the United States Government or any agency thereof.